Postprint of: Tarasiuk W., Golak K., Tsybrii Y., Nosko O., Correlations between the wear of car brake friction materials and airborne wear particle emissions, Wear, Vol. 456–457 (2020), 203361, DOI: 10.1016/j.wear.2020.203361

Correlations between the wear of car brake friction materials and airborne wear particle emissions

Wojciech Tarasiuk[1], Karol Golak[1], Yurii Tsybrii[1], Oleksii Nosko[1*]

[1] Bialystok University of Technology, Faculty of Mechanical Engineering,
ul. Wiejska 45C, Bialystok 15-351, Poland
[*]Corresponding author: o.nosko@pb.edu.pl (O. Nosko)

Keywords: sliding contact, friction material, wear, wear particles, airborne particles

Airborne wear particles emitted from transport vehicle brakes are one of the main sources of toxic metals in inhalable particulate matter. Prediction of wear particle emissions may become more accurate if the relationship between the wear and particle emission characteristics is known. An experimental study was performed to investigate proportional correlations between the mass wear, 0.01–0.42 μm particle emission measured by a NanoScan SMPS Nanoparticle Sizer (SMPS) and 0.3–10 μm particle emission measured by an Optical Particle Sizer (OPS). Several car brake low-metallic materials in the form of pin samples were tested against steel disc samples at different values of the contact pressure and sliding velocity. The pin-on-disc friction pair was placed in a clean chamber to eliminate external particle sources. The obtained results suggest a strong proportional correlation between the disc sample wear and pin sample wear. OPS and SMPS particle concentrations were also revealed to strongly correlate between each other. By contrast, the disc sample wear exhibited weak correlations with the particle concentrations for most of the materials.

1. Introduction

It is well known that airborne particulate matter is the cause for the occurrence of various diseases and reduction of lifespan. According to the statistical report [1] (p.40–45) of the World Health Organisation, atmospheric pollution is responsible for millions of deaths on our planet every year. The concentration and properties of atmospheric pollutants depend on the natural factors, e.g. wildfires, volcanic eruptions, topographic and climatic conditions, as well as on the anthropogenic factors including power plants, industrial facilities, agricultural areas and transport. The contribution of the latter is especially significant in urban areas and in the vicinity of highways where a huge number of transport vehicles are continuously in service (Furusjö et al. [2], Querol et al. [3]).

The traffic-related sources of airborne particles are classified into two basic groups: exhaust emissions due to the fuel combustion; non-exhaust emissions caused by the wear of brakes, tyres, road surfaces and by road dust resuspension (Thorpe and Harrison [4]). Air quality measurements revealed that the non-exhaust sources contribute a large amount of PM10 (mass concentration of particles smaller than 10 μm) and can even predominate over the exhaust ones in specific regions (Ketzel et al. [5]). Here wear particle emissions from brakes are of special attention since they constitute a major source of toxic metals in inhalable particulate matter (Gielt et al. [6], Gasser et al. [7]).

Many studies have been reported during the last two decades investigating wear emissions from the brakes of cars, trains and other transport vehicles, as reviewed by Grigoratos and Martini [8] and Kukutschová and Filip [9]. The common methodology of quantification of airborne wear particles implies the following research procedures: particle generation by using a tribometer or brake test stand or conducting tests in field; particle transportation from the friction contact to the sampling inlets of aerosol measurement instruments by creating an appropriate airflow; particle sampling, counting and collection by the aerosol measurement instruments. The measurement system should maximally eliminate external sources of particles so that the sampled particles originated from the friction contact. It should also provide high-efficiency sampling at which the measured particle concentration is related to the actual particle emission rate. Thereby, an experimental study of wear particle emissions requires parallel use of tribological and aerosol measurement equipment with the strict requirements to the particle measurement system, which leads to the necessity of application of theoretical methods.

Olofsson et al. [10] proposed a model to predict the number of airborne wear particles assuming that the particle generation rate is proportional to the load and inversely proportional to the hardness of the worn surface. A dimensionless *particle coefficient* was introduced as a proportionality coefficient indicating the probability that a generated particle becomes airborne.

Furthermore, it was shown that the particle coefficient and wear coefficient depend on the load in a similar way for steel-on-steel contacts, underlining a relationship between the particle emission and wear process. Thereby, the emission of wear particles was characterised by the particle coefficient, similarly as the wear process is characterised by the wear coefficient. This approach was subsequently improved by Wahlström et al. [11], Alemani et al. [12], Perricone et al. [13], Riva et al. [14].

Wahlström [15] simulated wear particle emissions from a disc brake coupled with the processes of mechanical deformations, wear, heat conduction and contact plateaus formation. The volume of the emitted particulate matter was assumed to be proportional to the total volume wear of the friction elements with an *airborne wear fraction* acting as a proportionality coefficient. This approach makes it possible to utilise wear test data for prediction of particle emissions and, accordingly, to substantially decrease the number of particle measurements. However, its applicability depends on the existence of correlations between the wear and particle emission characteristics.

Airborne particles are counted and size-classified using various aerosol measurement instruments. Depending on the operation principle and design, these instruments differ in their particle size measurement ranges (Giechaskiel et al. [16]). For instance, instruments that determine optical diameter of a particle based on its ability to scatter light have a lower measurement limit of order 0.1 μm. On the contrary, instruments that are designed to measure electrical mobility diameters of nanoparticles have an upper measurement limit of order 1 μm. Therefore, quantification of wear particle emissions covering a wide particle size range from nanometres to micrometres often involves application of two or more aerosol measurement instruments. If the particle concentration or another characteristic is measured only by one instrument, the question arises whether it can be extrapolated onto a size range of smaller or larger particles. This question is intimately related to the existence of correlations between the particle emission characteristics obtained by different aerosol measurement instruments.

As follows from the foregoing, prediction of wear particle emissions based on the utilisation of wear test data or extrapolation of particle emission data requires the existence of a relationship between the corresponding characteristics and knowledge of its properties. With this in mind, the purpose of the present study was to experimentally investigate proportional correlations between the mass wear and concentrations of 0.01–10 μm airborne wear particles measured by optical and electrical mobility aerosol instruments for several car brake friction materials in contact with a steel.

2. Experimental study

2.1. Tribological measurements

The study was performed using a T-11 pin-on-disc tribometer produced by the Institute for Sustainable Technologies in Radom (Poland). The pin sample had diameter 8 mm and length 8 mm. It was pressed by a dead weight against a disc sample, with contact pressure p. The disc sample, with diameter 60 mm and thickness 6.5 mm, was rigidly mounted on a disc support by a screw. The disc support in its turn was driven by a motor with constant angular velocity. The distance between the axis of the disc sample and that of the pin sample was 20 mm. The sliding velocity at this distance was equal to v. The friction force was measured by an HBM S2 force transducer with resolution 0.01 N. The friction coefficient μ was calculated as the ratio of the friction force to the dead weight load on the pin sample.

A chromel–alumel thermocouple (K type) measured temperature T in the pin sample. The measuring junction of the thermocouple had spherical shape of diameter 0.25 mm. It was installed into a 0.6 mm diameter blind hole drilled in the pin sample along its axis at distance 2 mm from the friction surface. The thermocouple signal was sampled by a Graphtech GL7000/GL7-HSV data logger at frequency 1 Hz.

The mass wear w_{pin} and w_{disc} of the pin and disc samples were determined by their weighting before and after the test. A Radwag XA 210.4Y.A analytical balance with resolution 0.01 mg was used for this purpose. To maximise the measurement accuracy, installation and dismantling of the pin and disc samples were done carefully, without altering their surfaces. Before the weighting, the samples were blown by air to remove dust or settled wear matter.

2.2. Particle emission measurements

To eliminate all external sources of particles, the friction pair of the pin-on-disc tribometer was placed in a clean chamber of volume 0.55 L, as illustrated in Fig.1. A Bambi PT50D compressor pumped air into a 50 L receiver to maintain pressure of above 6 bar. The air flowed then from the receiver to a 30 mm diameter chamber inlet via a TSI Filtered Air Supply 3074B system that removed particles with nominal efficiency 99.99995% at 0.1 μm and water vapour. The chamber inlet airflow, measured by a TSI Flow Calibrator 4048, was 6.2±0.2 L/min. Wear particles emitted from the friction contact were absorbed by the air inside the chamber. The air was sampled by a TSI NanoScan SMPS Nanoparticle Sizer 3910 (SMPS) and a TSI Optical Particle Sizer 3330 (OPS) with nominal flow rates 0.75 L/min and 1 L/min, respectively. The inlets of SMPS and OPS were connected to a 30 mm diameter chamber outlet by silicon tubes with internal diameter 6 mm and length 200 mm.

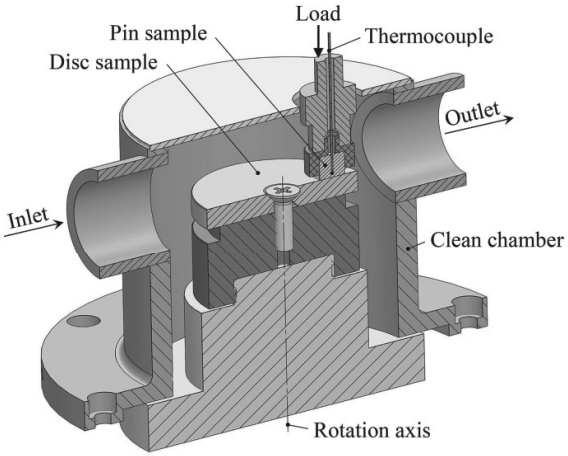

Fig.1. Schematic of the pin-on-disc friction pair in the clean chamber

SMPS allows classification of 10–420 nm particles by size. Its operation involves charging particles by a unipolar charger, selecting particles of specific diameter ranges by a radial differential mobility analyser, and counting particles by an isopropanol-based condensation particle counter. Particles are classified into 13 stages with midpoints 11.5, 15.4, 20.5, 27.4, 36.5, 48.7, 64.9, 86.6, 116, 154, 205, 274, 365 nm with frequency of 1 min^{-1}. OPS provides classification of 0.3–10 µm particles into 16 stages with midpoints 0.337, 0.419, 0.522, 0.65, 0.809, 1.01, 1.25, 1.56, 1.94, 2.42, 3.01, 3.75, 4.67, 5.82, 7.24, 9.02 µm with frequency 1 Hz. Based on the mentioned size distributions, SMPS and OPS calculate number particle concentrations C_{SMPS} and C_{OPS}, expressed in no/cm^3, and volume particle concentrations V_{SMPS} and V_{OPS}, expressed in $\mu m^3/cm^3$. The combination of SMPS and OPS enables thus quantification of 10 nm to 10 µm particles.

Before each test, systematic calibration and cleaning procedures were carried out. The parameters of SMPS and OPS were checked to be within allowable ranges. The clean chamber, relevant components of the pin-on-disc tribometer, silicon tubes and SMPS inlet cyclone were carefully cleaned. The particle concentrations C_{SMPS} and C_{OPS} were checked just before the test start in the absence of friction. C_{SMPS} was below 100 no/cm^3, while C_{OPS} was zero.

2.3. Friction materials

Pin samples were milled out from the friction pads used in the disc brakes of passenger cars. The friction pads were manufactured by 6 friction material companies and sold in price range 40–55 € per set of 4 pads. The friction pad materials were code-named C1 to C6. The milling was performed using a 6040T4D milling machine equipped with a numerical control system. During the

milling process, the friction surface of the pin sample was not altered. Moreover, no overheating of the pin sample was provided to preserve its original properties. Disc samples were manufactured from 42CrMo3 steel used for tribological applications.

Table 1 presents elemental compositions of the pin and disc samples obtained by energy-dispersive X-ray spectroscopy. It is seen that the iron content in the pin samples makes up 10–22 wt%, i.e. the pin sample materials belong to the class of low-metallic friction materials. Two of the pin sample materials, namely, C1 and C4, include copper content.

Table 1. Elemental compositions of the pin and disc samples, wt%

Element	Pin sample						Disc sample
	C1	C2	C3	C4	C5	C6	
C	39.8	36.4	47.8	47.2	38.7	50.9	0.3
O	16.5	24	20.6	18.3	17	11.8	
Mg	0.4	2.2	0.8	0.8	0.7	2.3	
Al	0.8	1.3	2.8	3	3.8	3.5	
Si	0.7	3.3	1.8	2.6	1.6	0.4	0.1
S	2.6	6	2.3	2.6	3.7	3.9	
K		0.5	0.1	0.2	0.1		
Ca		1.1	5.1	1.9	6	2.3	
Cr					0.5	1.5	1.2
Mn	0.1		0.7		1.4		0.9
Fe	17	10.5	12.2	14.4	21.6	14.2	97
Ni							0.2
Cu	4.4			1.2			0.1
Zn	1.6		1.9		1.2	3.2	
Mo							0.2
Sb	7.5						
Ba	8.6	14.7	3.9	7.8	3.7	6	

2.4. Friction conditions

Each test was conducted with a new pair of samples under constant contact pressure p and sliding velocity v. The test duration was 120 min. The room temperature was 22±2 °C. The relative humidity in the room was 35±5%.

Figure 2 shows the typical results obtained from a single test. Running-in processes took place manifesting themselves in unexpected changes in the friction coefficient μ and particle concentrations C_{SMPS} and C_{OPS}. These processes stabilised with time t, and the measured characteristics reached their stationary values. For definiteness, the stationary values were calculated by averaging on the interval of 60–120 min.

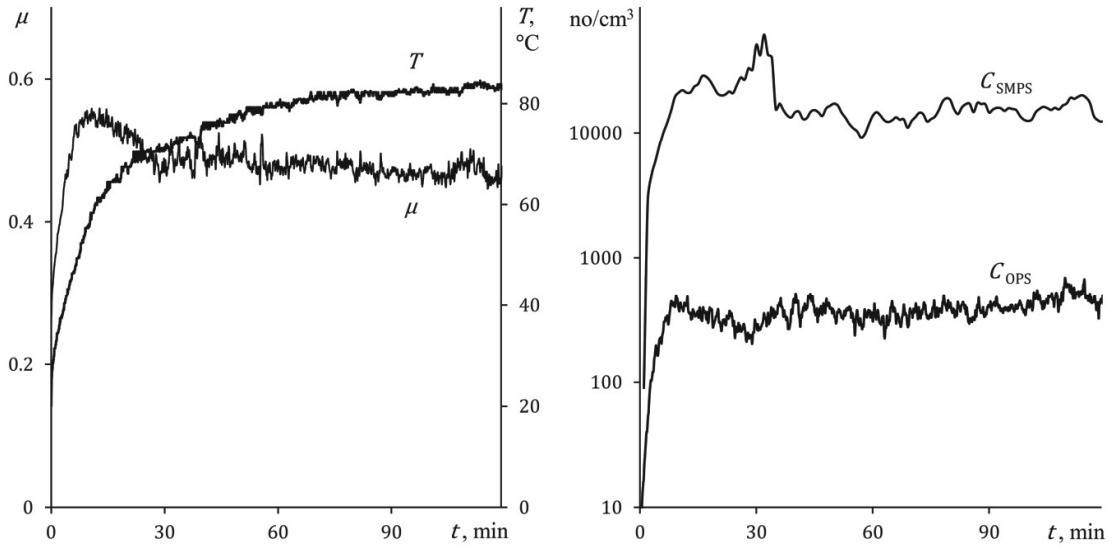

Fig.2. Typical test results (C1, 0.66 MPa × 1.2 m/s)

2.5. Experimental design

In the study, the controlled input variables are p and v, while the stationary values of μ, T, C_{SMPS}, C_{OPS}, V_{SMPS} and V_{OPS} serve as output variables. In order to cover wide ranges of the output variables, 3 levels of p were combined with 3 levels of v to give 9 different loading regimes $p \times v$, namely, 0.33 MPa × 0.6 m/s (lightest), 0.33 MPa × 1.2 m/s, 0.33 MPa × 1.8 m/s, 0.66 MPa × 0.6 m/s, 0.66 MPa × 1.2 m/s, 0.66 MPa × 1.8 m/s, 1 MPa × 0.6 m/s, 1 MPa × 1.2 m/s, 1 MPa × 1.8 m/s (heaviest). For each loading regime, a basic test and a retest were conducted. The retest data were compared with the basic test data to estimate the test–retest reliability.

The influence of uncontrolled factors on the output variables was minimised by providing the same conditions for all tests including the environmental conditions (temperature, relative humidity, clean chamber inlet airflow), equipment settings (tribometer, analytical balance, SMPS, OPS), experimental procedures (sample installation and dismantling, sample weighting, clean chamber cleaning) and operator.

The relationship between the output variables was analysed using the following approach. Consider a series of n measurements of two variables (x_i, y_i) indexed by $i = 1,2,\ldots,n$. Further,

assume that y_i is proportional to x_i. The correlation between x_i and y_i can be then described using the uncentered coefficient of determination

$$r^2 = 1 - \sum_{i=1}^{n} (y_i - kx_i)^2 \Big/ \sum_{i=1}^{n} y_i^2$$

where the proportionality coefficient k is determined by the method of least squares:

$$k = \sum_{i=1}^{n} (x_i y_i) \Big/ \sum_{i=1}^{n} x_i^2$$

The coefficient r^2 defined above characterises the degree of proportionality between x_i and y_i. It varies from zero (no proportional correlation) to 1 (absolute proportionality). In addition, the accuracy of the proportional model is indicated by the mean absolute relative deviation

$$\varepsilon = \frac{1}{n} \sum_{i=1}^{n} \left| 1 - \frac{kx_i}{y_i} \right|$$

Obviously, the smaller is the value of ε, the higher accuracy is attained.

3. Results

The experimental results obtained from the basic tests are represented in the form of bar diagrams. Each diagram describes a certain characteristic for all materials and loading regimes, which enables easy comparisons.

3.1. Tribological results

Figure 3 presents the stationary values of the friction coefficient μ. For all materials, μ lies in between 0.38 and 0.76. It is seen that μ generally decreases with increasing sliding velocity v.

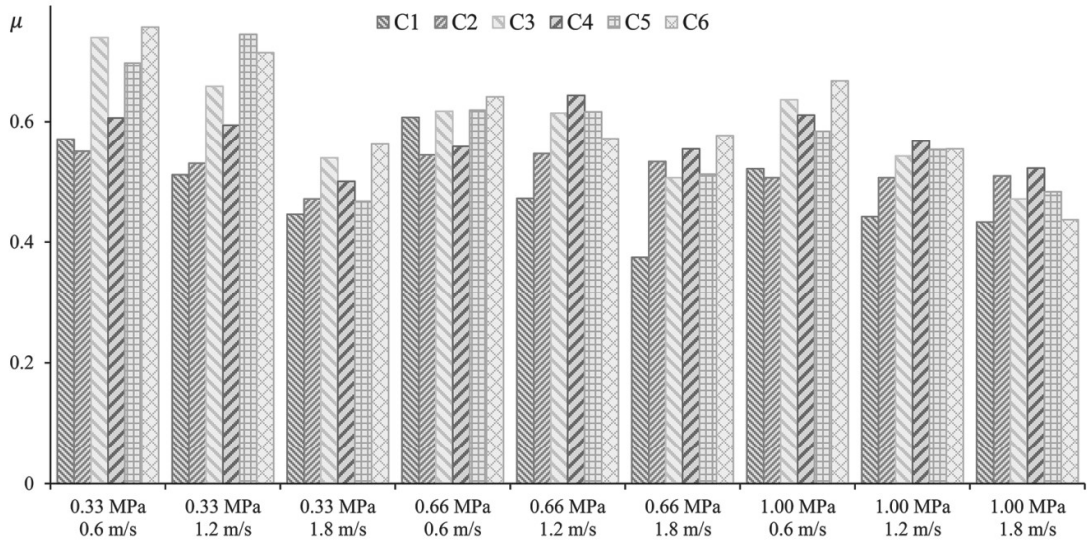

Fig.3. Stationary values of the friction coefficient μ

Figure 4 shows the stationary values of the pin sample temperature T. For the lightest loading regime 0.33 MPa × 0.6 m/s, T is about 40 °C. As one may expect, T increases as the loading intensifies. For the heaviest loading regime 1 MPa × 1.8 m/s, T is about 150 °C.

Nosko et al. [17] investigated low-metallic and non-asbestos organic car brake materials and revealed that an intensive nucleation of 1.3–40 nm particles occurs as temperature exceeds the level of 160 °C, which has a drastic effect on the particle emission characteristics. Since T is below the mentioned level, airborne particles observed in the present study most probably originate solely from the wear process.

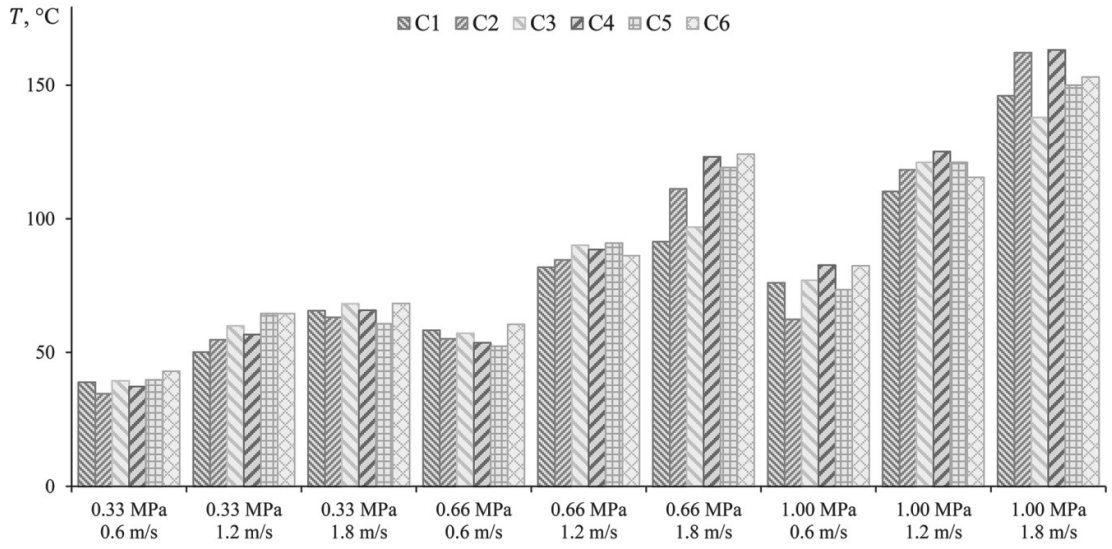

Fig.4. Stationary values of the pin sample temperature T

Figure 5 shows the mass wear w_{pin} and w_{disc} of the pin and disc samples. At the lighter loading regimes, when p=0.33 MPa or v=0.6 m/s, w_{pin} and w_{disc} generally increase with an increase in p or v. However, at the heavier loading regimes, they exhibit different trends. For most of the materials, w_{pin} and w_{disc} decrease as v changes from 1.2 to 1.8 m/s at p equal to 0.66 or 1 MPa. The test–retest variability of w_{pin} and w_{disc} is below 10%.

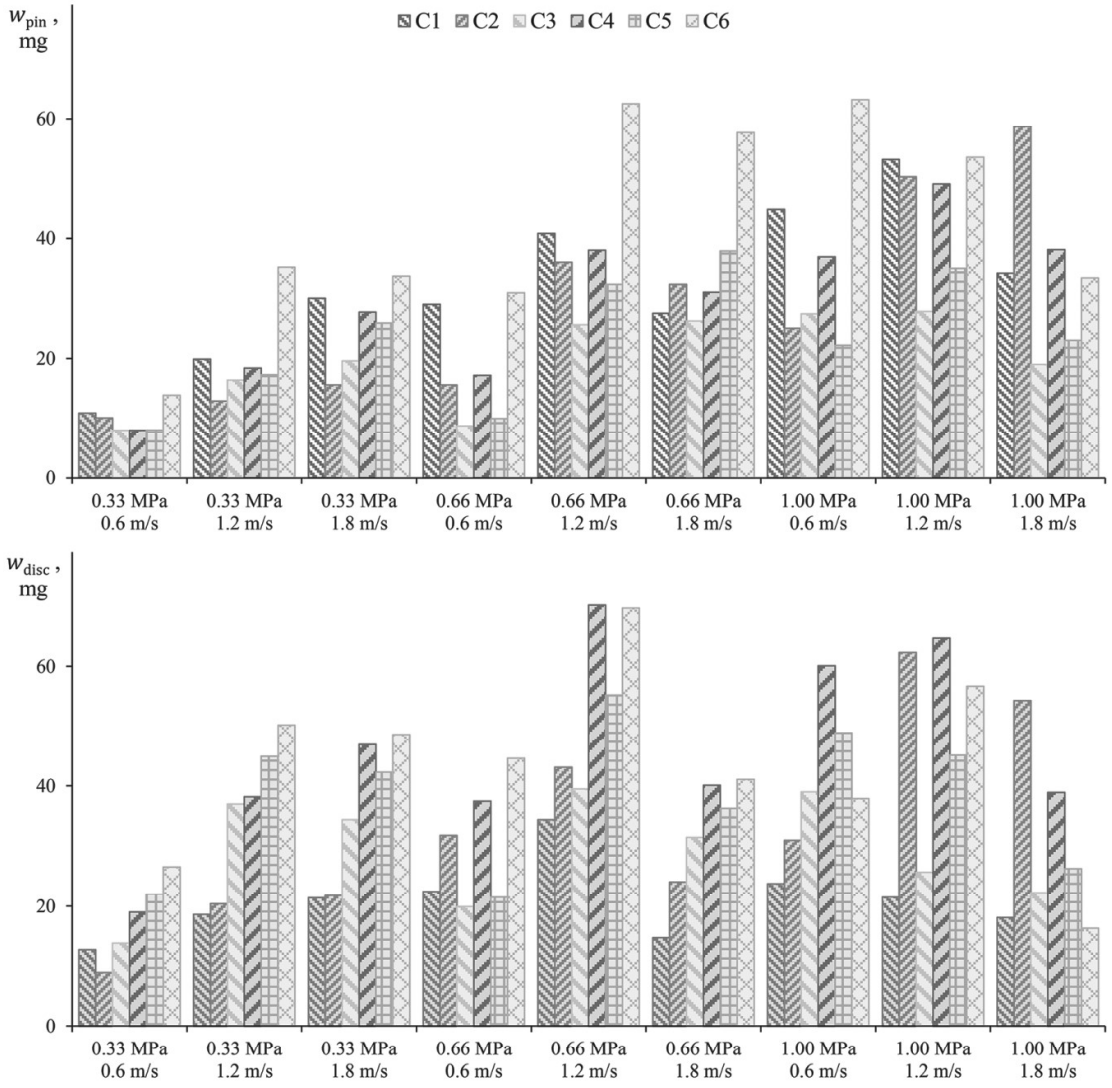

Fig.5. Pin sample mass wear w_{pin} and disc sample mass wear w_{disc}

3.2. Particle emission results

Figure 6 presents the stationary values of the particle concentrations C_{SMPS} and C_{OPS}. It is shown that C_{SMPS} takes values of order 10^3 to 10^4 no/cm^3, while C_{OPS} is of order 10^2 to 10^3 no/cm^3. The test–retest variability of C_{SMPS} and C_{OPS} is about 30%.

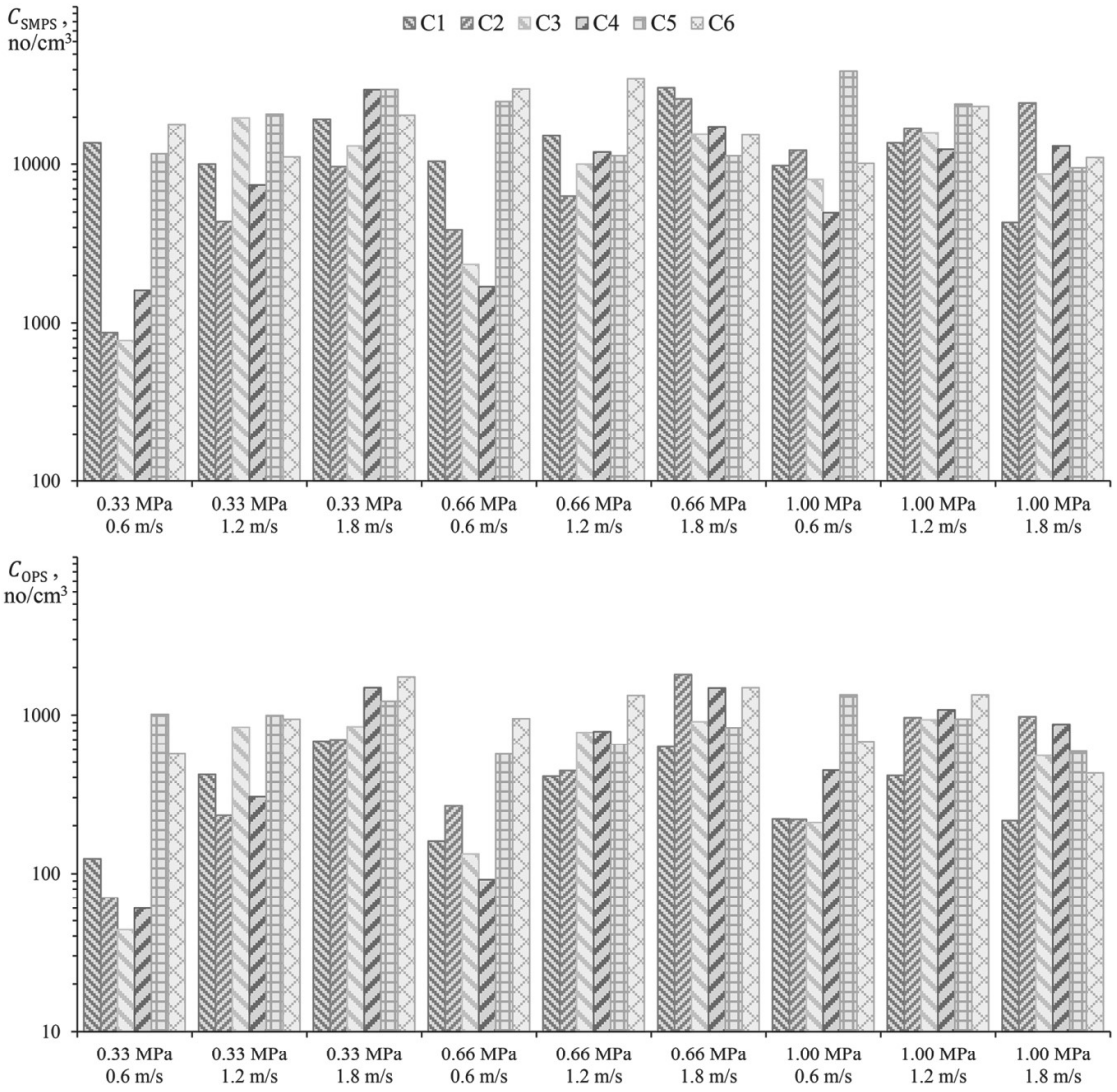

Fig.6. Stationary values of the number particle concentrations C_{SMPS} and C_{OPS}

Figure 7 shows the stationary concentrations this time expressed in terms of particulate matter volume V_{SMPS} and V_{OPS}. The values of V_{SMPS} are of order 10 to 10^2 μm^3/cm^3, whereas those of V_{OPS} are significantly larger of order 10^2 to 10^3 μm^3/cm^3.

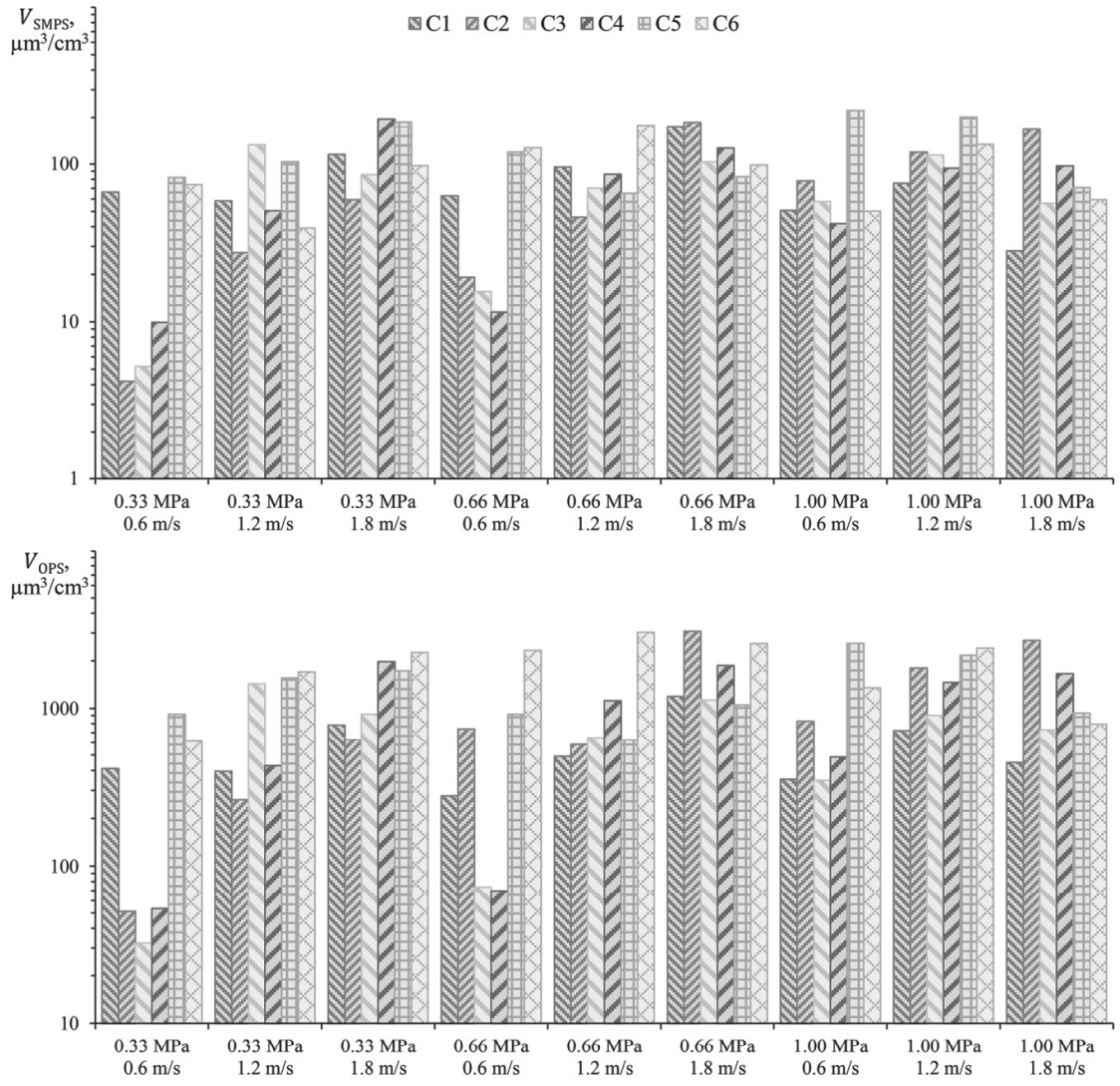

Fig.7. Stationary values of the volume particle concentrations V_{SMPS} and V_{OPS}

Figure 8 shows how the particles are distributed by size d for the lightest (a) and heaviest (b) loading regimes. In case (a), SMPS distribution has a peak at 0.09–0.21 µm, while OPS distribution has a predominating peak at 0.42–0.52 µm and a smaller one at 1.56–1.94 µm. As the loading intensifies, the SMPS distribution peak shifts in the direction of larger particles to 0.27–0.37 µm, whereas the locations of the two OPS distribution peaks are not affected, as shown in case (b). Such a behaviour suggests that in case (b) the closely located SMPS distribution peak (0.27–0.37 µm) and OPS distribution peak (0.42–0.52 µm) correspond to different particles. It should be noted that a similar behaviour of size distributions of brake wear particles was previously reported by Alemani et al. [18].

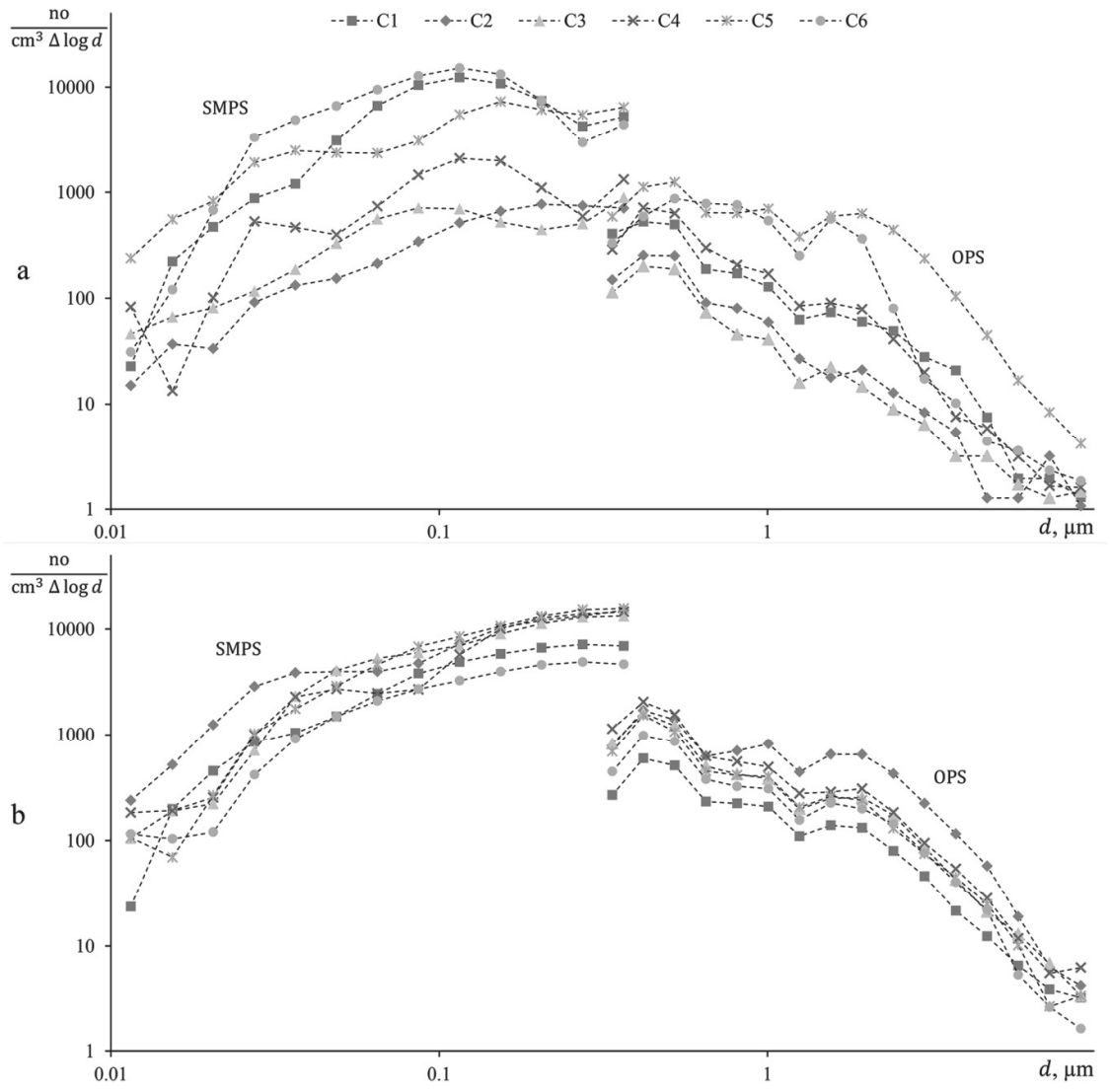

Fig.8. SMPS and OPS particle size distributions:
(a) lightest loading regime 0.33 MPa × 0.6 m/s; (b) heaviest loading regime 1 MPa × 1.8 m/s

4. Analysis and discussion

First, analyse the relationship between the disc sample wear w_{disc} and pin sample wear w_{pin}. Fig.9 provides the relevant results. In this and following figures, the left plot indicates the experimental points and a fitted line with the slope k for each material. The right plot shows the corresponding percent values of r^2 and ε. According to the results, there is a strong correlation between w_{disc} and w_{pin} for all materials with r^2=92±3% and ε=30±5%. The slope k varies between 0.61 (C5) and 1.52 (C1), implying that the disc and pin samples are worn out in a relatively close mass proportion. Note that larger values of w_{disc} and w_{pin} do not necessarily correspond to a heavier loading regime, as mentioned in Section **3.1**.

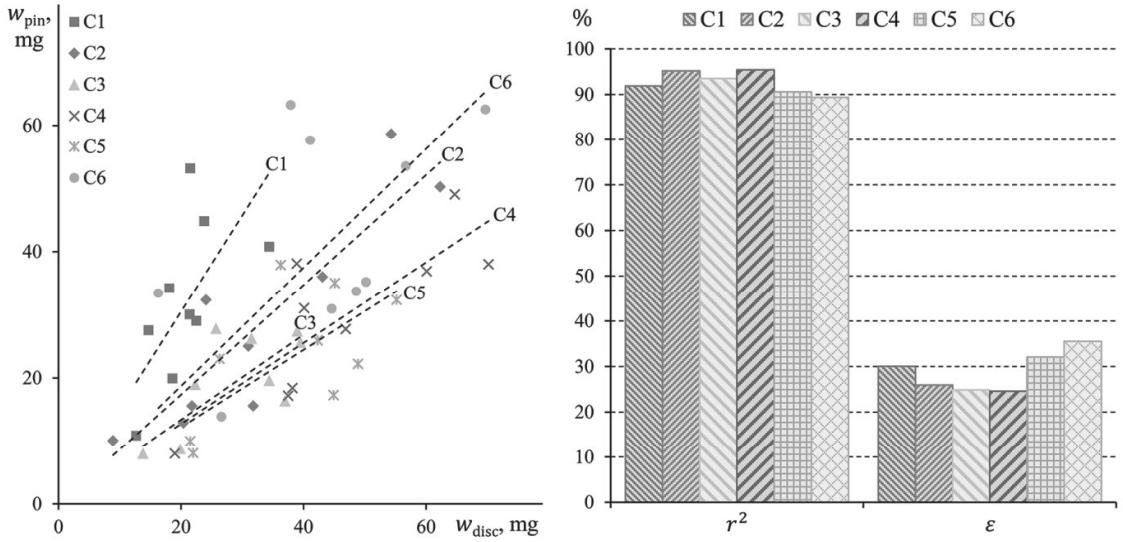

Fig.9. Correlation between the disc sample wear w_{disc} and pin sample wear w_{pin}

The relationship between the particle concentrations C_{OPS} and C_{SMPS} is depicted in Fig.10. The correlation between the concentrations is strong, with r^2=90±5% and ε=27±10%. The slope k approximately equals 14 for C4, 17 for C2, C3, C6, 23 for C5, and 36 for C1. Thereby, SMPS detects 14–36 particles per 1 particle detected by OPS.

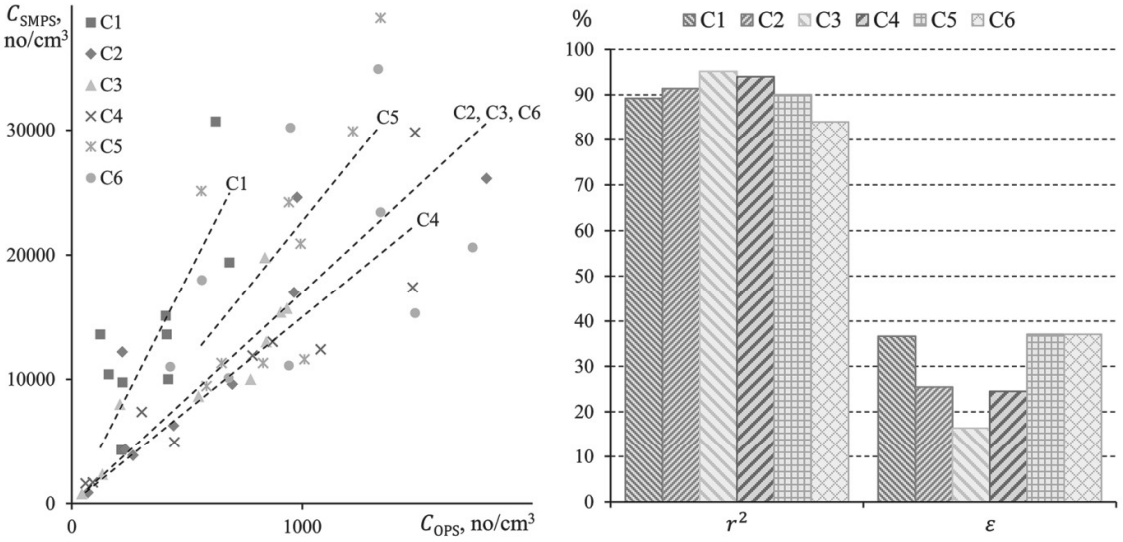

Fig.10. Correlation between the number particle concentrations C_{OPS} and C_{SMPS}

The volume particle concentrations V_{OPS} and V_{SMPS} are interrelated as presented in Fig.11. Here a strong correlation is seen, similarly to that in Fig.10. The calculations show that r^2=95±2%

and ε=25±10%, while k takes values between 0.05 (C6) and 0.14 (C1), i.e. 1 μm^3 of SMPS-registered particulate matter corresponds to 7–20 μm^3 of OPS-registered one.

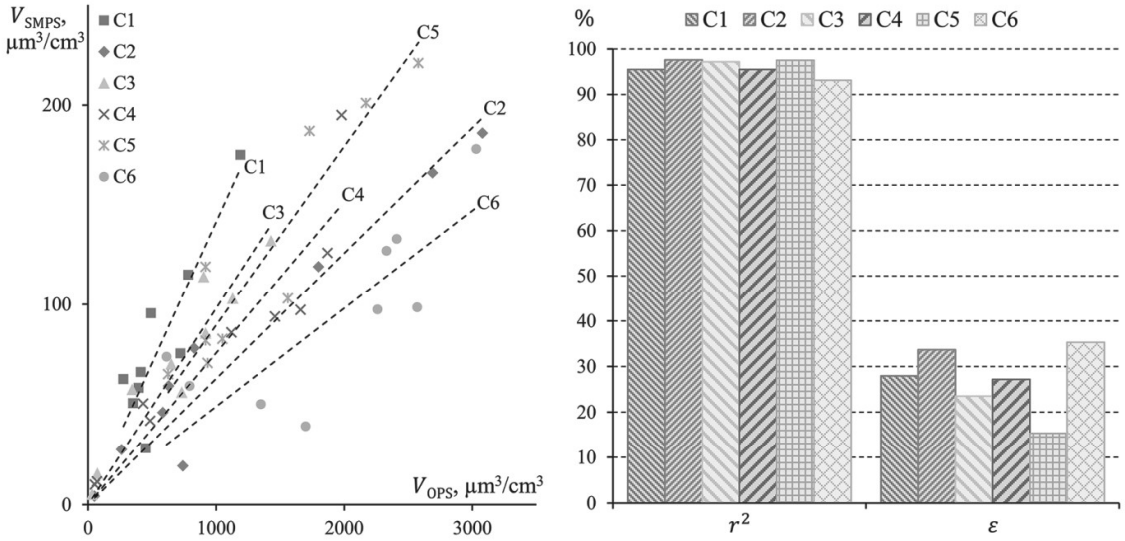

Fig.11. Correlation between the volume particle concentrations V_{OPS} and V_{SMPS}

The results in Fig.10 and Fig.11 suggest that OPS concentration (C_{OPS}) of 0.3–10 μm particles can be extrapolated onto the smaller particle size range of 0.01–0.42 μm covered by SMPS with error (ε) of about 27%. It is remarkable that the proportional correlation between V_{OPS} and V_{SMPS} (r^2≈95%), calculated based on the respective particle size distributions, is stronger than that between C_{OPS} and C_{SMPS} (r^2≈90%).

Finally, consider the relationship between the wear and particle concentrations. Fig.12 presents the relevant results for w_{disc} vs C_{SMPS}. A large scatter is seen in the locations of the experimental points. The coefficient r^2 is below 85% for all materials except for C6. The deviation ε exceeds 55% for most of the materials. This allows to conclude that the proportional correlation is weak.

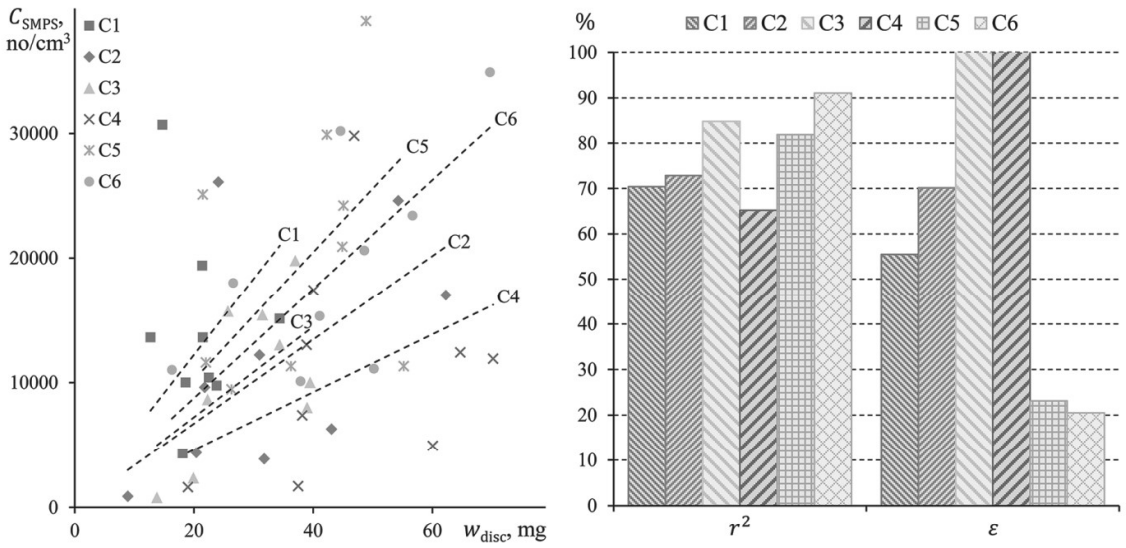

Fig.12. Correlation between the disc sample wear w_{disc} and particle concentration C_{SMPS}

A similar weak correlation holds between w_{disc} and C_{OPS}, as shown in Fig.13. Most of the materials have r^2 below 82%. The deviation ε is above 44% except for C6. Note that the variation range of the slope k is noticeably narrower compared to that intrinsic to the relationship between w_{disc} and C_{SMPS} in Fig.12.

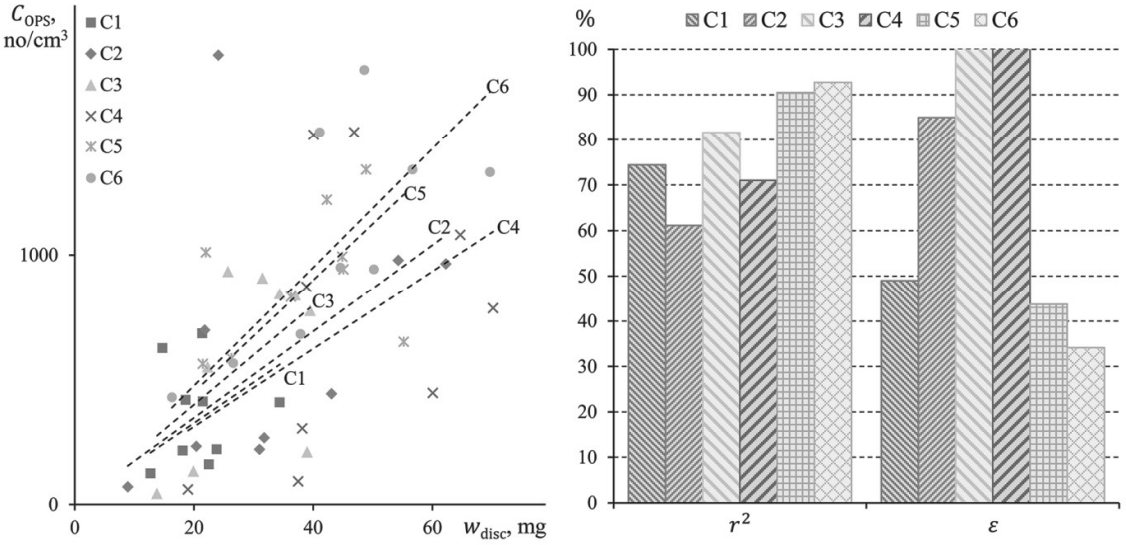

Fig.13. Correlation between the disc sample wear w_{disc} and particle concentration C_{OPS}

The results in Fig.12 and Fig.13 show that both C_{SMPS} and C_{OPS} correlate weakly with w_{disc}, implying that the wear particle emission cannot be generally predicted based solely on the wear test data. Nonetheless, strong correlations are revealed between the mentioned characteristics for

material C6. It holds that r^2=91% and ε=21% for w_{disc} vs C_{SMPS} and r^2=93% and ε=34% for w_{disc} vs C_{OPS}. This leads to the hypothesis that there is a class of friction pairs that exhibit a proportional relationship between the wear and particle emission characteristics. Further studies are needed here.

5. Conclusion

A pin-on-disc study of 6 car brake low-metallic materials was performed aimed at the identification of proportional correlations between the mass wear and emissions of 0.01–10 μm airborne wear particles. The clean chamber approach was applied for accurate counting and size classification of wear particles by NanoScan SMPS Nanoparticle Sizer 3910 (SMPS) and Optical Particle Sizer 3330 (OPS). The main findings can be summarised as follows:

1. There is a strong proportional correlation between the disc sample wear and pin sample wear with the uncentered coefficient of determination r^2≈92%.
2. There is a strong proportional correlation between OPS and SMPS number particle concentrations with r^2≈90%. OPS number concentration of 0.3–10 μm particles can be extrapolated onto the smaller particle size range of 0.01–0.42 μm covered by SMPS with error ε ≈27%.
3. There is a strong proportional correlation between OPS and SMPS volume particle concentrations with r^2≈95%. This correlation is stronger than that between OPS and SMPS number particle concentrations.
4. Generally, the wear correlates weakly with the particle emission characteristics. Only for 1 of the 6 materials, the disc sample wear correlates strongly with SMPS number particle concentration (r^2=91%, ε=21%) and OPS number particle concentration (r^2=93%, ε=34%).

The present work was supported by the National Science Centre, Poland [grant number 2017/26/D/ST8/00142].

References

[1] World health statistics 2019: monitoring health for the SDGs, sustainable development goals. Geneva: World Health Organization; 2019.

[2] E. Furusjö, J. Sternbeck, A.P. Cousins, PM10 source characterization at urban and highway roadside locations, Science of the Total Environment 387 (1–3) (2007) 206–219.

[3] X. Querol, A. Alastuey, C.R. Ruiz, B. Artiñano, H.C. Hansson, R.M. Harrison, E. Buringh, H.M. ten Brink, M. Lutz, P. Bruckmann, P. Straehl, J. Schneider, Speciation and origin of

PM10 and PM2.5 in selected European cities, Atmospheric Environment 38 (2004) 6547–6555.

[4] A. Thorpe, R.M. Harrison, Sources and properties of non-exhaust particulate matter from road traffic: A review, Science of the Total Environment 400 (1–3) (2008) 270–282.

[5] M. Ketzel, G. Omstedt, C. Johansson, I. Düring, M. Pohjola, D. Oettl, L. Gidhagen, P. Wåhlin, A. Lohmeyer, M. Haakana, R. Berkowicz, Estimation and validation of PM2.5/PM10 exhaust and non-exhaust emission factors for practical street pollution modelling, Atmospheric Environment 41 (40) (2007) 9370–9385.

[6] J.K. Gietl, R. Lawrence, A.J. Thorpe, R.M. Harrison, Identification of brake wear particles and derivation of a quantitative tracer for brake dust at a major road, Atmospheric Environment 44 (2) (2010) 141–146.

[7] M. Gasser, M. Riediker, L. Mueller, A. Perrenoud, F. Blank, P. Gehr, B. Rothen-Rutishauser, Toxic effects of brake wear particles on epithelial lung cells in vitro, Particle and Fibre Toxicology 6 (2009) 30.

[8] T. Grigoratos, G. Martini, Brake wear particle emissions: a review, Environmental Science and Pollution Research 22 (4) (2015) 2491–2504.

[9] J. Kukutschová, P. Filip, Review of brake wear emissions: A review of brake emission measurement studies: Identification of gaps and future needs, in: F. Amato (Ed.), Non-exhaust emissions, Academic Press, 2018, pp.123–146.

[10] U. Olofsson, L. Olander, A. Jansson, Towards a model for the number of airborne particles generated from a sliding contact, Wear 267 (12) (2009) 2252–2256.

[11] J. Wahlström, A. Söderberg, U. Olofsson, Simulation of airborne wear particles from disc brakes, SAE Technical Paper (2009) 2009-01-3040.

[12] M. Alemani, J. Wahlström, U. Olofsson, On the influence of car brake system parameters on particulate matter emissions, Wear 396–397 (2018) 67–74.

[13] G. Perricone, V. Matějka, M. Alemani, G. Valota, A. Bonfanti, A. Ciotti, U. Olofsson, A. Söderberg, J. Wahlström, O. Nosko, G. Straffelini, S. Gialanella, M. Ibrahim, A concept for reducing PM10 emissions for car brakes by 50%, Wear 396–397 (2018) 135–145.

[14] G. Riva, G. Valota, G. Perricone, J. Wahlström, An FEA approach to simulate disc brake wear and airborne particle emissions, Tribology International 138 (2019) 90–98.

[15] J. Wahlström, A comparison of measured and simulated friction, wear, and particle emission of disc brakes, Tribology International 92 (2015) 503–511.

[16] B. Giechaskiel, M. Maricq, L. Ntziachristos, C. Dardiotis, X. Wang, H. Axmann, A. Bergmann, W. Schindler, Review of motor vehicle particulate emissions sampling and

measurement: From smoke and filter mass to particle number, Journal of Aerosol Science 67 (2014) 48–86.

[17] O. Nosko, J. Vanhanen, U. Olofsson, Emission of 1.3–10 nm airborne particles from brake materials, Aerosol Science and Technology 51 (1) (2017) 91–96.

[18] M. Alemani, O. Nosko, I. Metinoz, U. Olofsson, A study on emission of airborne wear particles from car brake friction pairs, SAE International Journal of Materials and Manufacturing 9 (1) (2016) 147–157.